INT. J. REMOTE SENSING, 20 FEBRUARY, 2004,
VOL. 25, NO. 4, 819–838

Taylor & Francis
Taylor & Francis Group

Estimating fragmentation effects on simulated forest net primary productivity derived from satellite imagery

N. C. COOPS†, J. D. WHITE‡§ and N. A. SCOTT‡¶

†CSIRO Forestry and Forest Products, Private Bag 10, Clayton South, 3169, Australia; e-mail: nicholas.coops@csiro.au
‡Landcare Research, Private Bag 11052, Palmerston North, New Zealand

(*Received 30 January 2002; in final form 12 March 2003*)

Abstract. Conversion of native forests to agriculture and urban land leads to fragmentation of forested landscapes with significant consequences for habitat conservation and forest productivity. When quantifying land-cover patterns from airborne or spaceborne sensors, the interconnectedness of fragmented landscapes may vary depending on the spatial resolution of the sensor and the extent at which the landscape is being observed. This scale dependence can significantly affect calculation of remote sensing vegetation indices, such as the Normalized Difference Vegetation Index (NDVI) and its subsequent use to predict biophysical parameters such as the fraction of photosynthetically active radiation intercepted by forest canopies (fPAR). This means that simulated above-ground net primary productivity (NPP_A) using canopy radiation interception models such as 3-PG (Physiological Principles for Predicting Growth), coupled with remote sensing observations, can yield different results in fragmented landscapes depending on the spatial resolution of the remotely sensed data.

We compared the amount of forest fragmentation in 1 km SPOT-4 VEGETATION pixels using a simultaneously acquired 20 m SPOT-4 multispectral (XS) image. We then predicted NPP_A for New Zealand native forest ecosystems using the 3-PG model with satellite-derived estimates of the fPAR obtained from the SPOT-4 VEGETATION sensor, using NDVI values with and without correction for fragmentation. We examined three methods to correct for sub-pixel fragmentation effects on NPP_A. These included: (1) a simple conversion between the broad 1 km scale NDVI values and the XS NDVI values; (2) utilization of contextural information from XS NDVI pixels to derive a single coefficient to adjust the 1 km NDVI values; and (3) calculation of the degree of fragmentation within each VEGETATION 1 km pixel and reduce NDVI by an empirically derived amount based on the proportional areal coverage of forest in each pixel. Our results indicate that predicted NPP_A derived from uncorrected 1 km VEGETATION pixels was significantly higher than estimates using adjusted NDVI values; all three methods reduced the predicted NPP_A. In areas of the landscape with a large

§Present address: Baylor University, Department of Biology, P.O. Box 97388, Waco, Texas 76798–7388, USA.

¶Present address: Woods Hole Research Center, P.O. Box 296, Woods Hole, Massachusetts 02543, USA.

International Journal of Remote Sensing
ISSN 0143-1161 print/ISSN 1366-5901 online
http://www.tandf.co.uk/journals
DOI: 10.1080/0143116031000115094

degree of forest fragmentation (such as forest boundaries) predictions of NPP_A indicate that the fragmentation effect has implications for spatially extensive estimates of carbon uptake by forests.

1. Introduction

The clearing of native forest for agriculture, pasture, harvesting or urban development can severely compromise the integrity of existing native ecological systems through loss of native species, invasion of exotic species, soil erosion, and changes in forest production (Forman and Godron 1986, Collinge 1996). This clearing of native scrub and forest also leads to landscape fragmentation when large, continuous areas of forests are divided into smaller blocks. Human-induced clearing of New Zealand forests was initiated by Polynesian migrants around 1000 BP, who reduced the total forest area by approximately 20% (Newsome 1987, Meurk and Swaffield 2000). Over the past 150 years, New Zealand's forest have continued to be cleared for agriculture and urban development, with many indigenous forests cleared for pasture. More recently, areas of pasture have been replaced by plantations of exotic species such as *Pinus radiata* and other commercially valuable species (Meurk and Swaffield 2000). Currently about 33% of the original indigenous forest area remains (Newsome 1987).

The fragmentation of native forest into smaller discrete blocks of remnant forest has a significant effect on the landscape by both increasing the perimeter of forest patches and changing the structural characteristics of the blocks themselves (Murcia 1995). For example, along edges of forest blocks, light availability is often elevated, leading to increased production (Young and Mitchell 1993). However, edge lengthening also increases the vulnerability of trees to wind. As a result the size and placement of remnant forest blocks within the landscape can have a significant impact on the habitat and forest productivity across the forest (Collinge 1996).

New Zealand, like many countries, is developing an understanding of their national carbon budget using a variety of methods to quantify changes in carbon storage in forests and scrub vegetation (e.g. White *et al.* 2000, Hall *et al.* 2001). One approach utilizes production efficiency models that provide spatially explicit estimates of above-ground net primary productivity (NPP_A) based on plant physiological processes; these models can also be driven by satellite observations that provide information on vegetation canopies (Goetz *et al.* 1999). A number of studies have demonstrated that when broad-scale remotely sensed observations are coupled with vegetation process models, the aggregation of surface properties either through the inherent restrictions of sensor resolution or by direct data manipulation result in an over estimation of vegetation productivity (White and Running 1994, Pierce and Running 1995).

White *et al.* (2000) and Coops *et al.* (2002) applied a simple physiological model (3-PG; Physiological Principles for Predicting Growth) to estimate NPP_A of a number of vegetation types in New Zealand. The 3-PG model is typical of many vegetation process models in that it estimates gross primary production (P_G), a fraction of which becomes net primary production (NPP), which is then allocated to different vegetation components (constrained by temperature, water supply, and nutrition (Landsberg and Waring 1997)). The 3-PG model requires few parameters, which can be easily derived from literature or from field measurements (Landsberg

and Waring 1997, Coops *et al.* 1998). The monthly time step of the model requires average daily short-wave incoming radiation, mean vapour pressure deficits, temperature extremes, total monthly rainfall and estimates of soil water storage capacity and fertility. When coupled with remotely sensed observations, 3-PG uses the fraction of photosynthetically active radiation absorbed by the forest canopies (fPAR) to constrain carbon uptake. fPAR is estimated from a satellite-derived index, based on the normalized difference between reflectances measured in the near-infrared and red wavelengths, termed the Normalized Difference Vegetation Index (NDVI). Predictions by 3-PG of above-ground stem biomass for the New Zealand South Island ($r^2 = 0.82$), and total vegetation biomass for the entire country ($r^2 = 0.72$) were highly correlated with field estimates once key 3-PG parameters were calibrated for New Zealand vegetation (White *et al.* 2000). Estimates of NPP_A were also produced by the model coupled with satellite imagery obtained from the SPOT-4 VEGETATION sensor at 1 km spatial resolution. The coupled model predicted stand NPP_A for sites across both islands well ($r^2 = 0.80$) when compared with field estimates (Coops *et al.*, in press).

Regional and global simulations of NPP_A are most easily accomplished using remotely sensed data with high-temporal frequency and low spatial resolution (Moody 1998) such as the Advanced Very High Resolution Radiometer (AVHRR) 1.1 km or SPOT-4 VEGETATION 1 km sensors. However many of the factors controlling vegetation condition such as human-induced clearing for agriculture and urban development occur at fine spatial scales only apparent using high spatial resolution remote sensing instruments (Moody 1998) and not at the scales observed by most global observing satellites. Fine-scale remote sensing of fragmented forest landscapes reveals a mosaic of different land-cover classes whose degree of interconnectedness can change based on the grain and extent (scale) at which the landscape is being observed. For example, if the size of remnant fragments of forest vegetation is 10 ha, and the pixel resolution of the acquired image is 100 ha (the typical size of AVHRR), then the signal-averaging process of the land-cover classes within the 100 ha pixel is an important issue. This is often referred to as the spatial scaling effect (Chen 1999).

Our objective in this paper was to investigate the spatial scaling effect on simulated NPP_A at broad scales (1 km spatial resolution) using a coupled vegetation process model driven by satellite imagery. To do this, forest fragmentation was estimated from a unique dataset; simultaneously acquired 1 km SPOT-4 VEGETATION and 20 m SPOT-4 multispectral (XS) imagery. A number of different methods are proposed to adjust the 1 km SPOT-4 VEGETATION data to account for observed fragmentation in the 20 m XS imagery.

2. Background

Contextural indices capture structure and patterns of fragments or objects in an image and include metrics such as the number, size, shape, area and pattern of objects and the distance between objects (Mather 1987) and provide a measure of the average variability of discreet or continuous objects within a viewing window. The use of contexture as an index of variation is different to patch variance (degree of changes within a specified distance) within a pixel. Chen (1999) concluded that when quantifying scaling effects contextural parameters have a number of key advantages over variance parameters including:

1. that contexture is the major cause of variation in the remote sensing response;
2. it can be more easily obtained than variance information at high resolutions (such as area relationships); and
3. the scaling methodology using contextural parameters is generally simpler than variance-based methods.

An example of the difference in variance and contexture within a broad-scale pixel is shown in figure 1. In this figure we consider two broad-scale pixels (each approximating 1 km × 1 km, similar to a broad-scale pixel obtained from a low spatial resolution, high temporal resolution sensor) with nine individual sub-scene units of known land use. In this example, we consider the white pixels land and the black water. In both cases the variance of the 1 km pixel (assuming mean values of water and land) is the same. However, the mean land area covered by water is 22% in figure 1(*a*) versus 78% in figure 1(*b*). The contexture of each pixel (in this case, the area of water versus the area of land) is a better measure of sub-pixel structure than the internal variance.

Chen (1999) concluded that when a broad scale, large area pixel, contains two contrasting cover types (such as vegetation and open water), derived bio-physical variables (such as fPAR, or alternatively leaf area index (L)) can be over-predicted by up to 45% of the correct value depending on the water area fraction in the pixel. These biases depended on contexture and little on variance (Chen 1999). In boreal regions with numerous small water bodies, simulations (Chen 1999) showed that the most useful contextural parameter for quantifying the scaling effect in mixed pixels was the water area fraction within each degraded pixel. In New Zealand, the role of small water bodies is less important compared to the influence of land-cover pattern on broad-scale pixel response, as the native scrub land and forest of New Zealand are fragmented due to urban encroachment and conversion to agricultural land.

3. Study area

In order to investigate the spatial scaling effect on simulated NPP_A we selected a region (60 km × 60 km) containing most of the land-cover types found in New Zealand and covered a productivity and topographic gradient. Approximately 40%

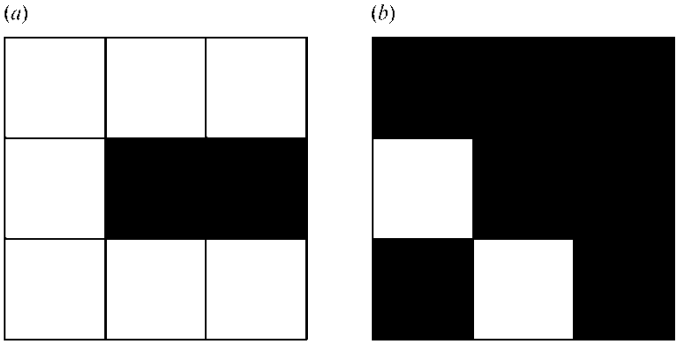

Figure 1. Schematic diagram of two 1 km × 1 km pixels with sub-pixel variation evident in the nine internal pixels. Each large pixel has the same internal variance but a markedly different contextural parameter.

of the region is native forest, with large areas of mountain beech forest (*Nothofagus solandrii*) ranging in biomass from 196 to 312 Mg DM ha^{1} (Hall *et al*. 2001) with small areas of exotic *Pinus radiata* plantations; an additional 40% of the area is pasture and arable land with the remainder low biomass scrub lands and snow covered grassland.

4. Input data

The SPOT-4 (Satellite Pour l'Observation de la Terre) satellite has two sensors: a high spatial resolution (20 m) multi-spectral imager (denoted as XS) which images in four spectral bands (blue: 0.43–0.47 μm, red: 0.61–0.68 μm, near-infrared: 0.78–0.89 μm and short-wave infrared: 1.58–1.75 μm) and the VEGETATION sensor which is analogous to the AVHRR sensor. The VEGETATION sensor has a spatial resolution of 1 km with daily image acquisition of the same location for sites above 35° north and south latitudes. Geometric accuracy of derived VEGETATION products is estimated at 350 m and simultaneous acquisition of high spatial resolution SPOT XS imagery (20 m) is possible.

One of our datasets consisted of two images acquired simultaneously on 5 January 1999 from the SPOT-4 satellite (figure 2). One image was obtained from the high spatial resolution XS sensor, and the other a single scene from the SPOT VEGETATION sensor (table 1). Both scenes were provided by CNES (Le Centre National d'Etudes Spatiales) in geometrically corrected form (with a stated spatial accuracy of less than half a pixel; 10 m for XS and 350 m for VEGETATION). The raw digital values of the two single SPOT-4 scenes were atmospherically corrected in an identical manner for path radiance due to atmospheric scattering using the clear lake method (Ahern *et al*. 1987). Average radiance values for the deep ocean surrounding both islands (for the VEGETATION image and off the coast on the XS image) were calculated and subtracted from the original radiance values. Neither scene was corrected for atmospheric transmissivity, as no ground-based data were available for the aerosol comparison covering the complete areas of both images. The NDVI was calculated for both images from the corrected band 3 and band 2 wavelengths where NDVI = (b3–b2)/(b3 + b2).

The second dataset consisted of 12 monthly composites of daily VEGETATION data at 1 km resolution collected over the 1998/9 growing season. These composite VEGETATION products were supplied and fully corrected for atmospheric and geometric effects by the VEGETATION program (see for additional data and specifications http://www.spotimage.fr/data/images/vege/vegetat/home.htm). This CNES calibration involved spectral band registration corrected for satellite location and altitude and terrain elevation.

Atmospheric correction was undertaken based on sensor-derived water vapour, ozone and aerosol parameters. The monthly composites of NDVI were then resampled onto the New Zealand Map grid.

The two images acquired on 5 January 1999 are shown in figure 2. Figure 2(*a*) shows the XS 20 m resolution NDVI image over the 60 km × 60 km study area, and figure 2(*b*) shows the VEGETATION 1 km NDVI image for the same region. The images show the study area with mixed land cover of predominantly forests, woodlands and pasture/agricultural land. The white regions in the VEGETATION image (high NDVI) in the south and west of the images are forested, with

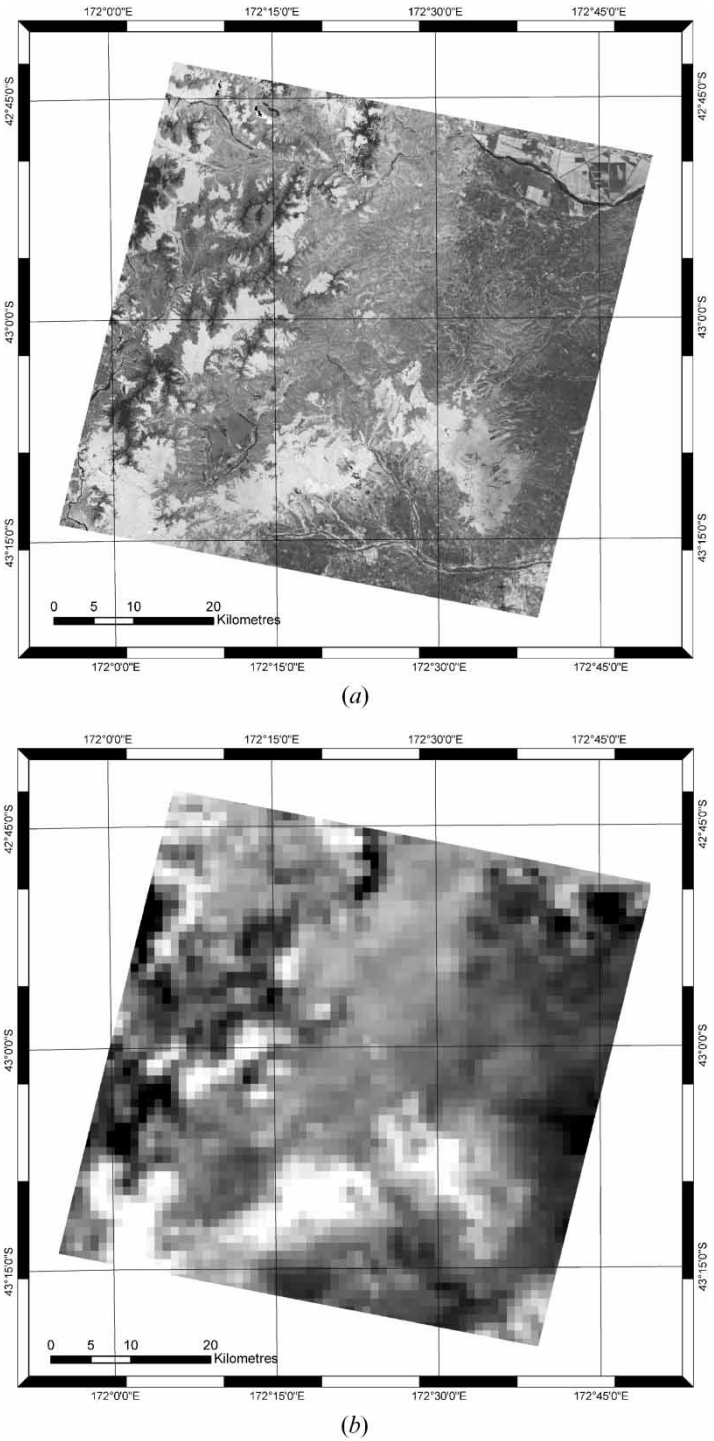

Figure 2. NDVI images at (*a*) 20 m spatial resolution from the XS sensor and (*b*) 1 km resolution from the VEGETATION sensor.

Table 1. Three scaling approaches to account for the spatial scaling effect on broad-scale imagery.

Technique	Description	Equation
Simple image fragmentation	Scale and discount VEGETATION NDVI by mean of 20 m values to account for contexture of other cover types.	New_NDVI (1 km) = VEGETATION_NDVI × mean 20 NDVI (figure 6)
Scene-based fragmentation	Compute mean fragmentation of each 60 km scene and reduce VEGETATION NDVI by a constant factor.	New_NDVI (1 km) = VEGETATION_NDVI × scene fragmentation value (obtained from figure 4)
Pixel-based fragmentation	Compute mean fragmentation in each 1 km cell of the scene and reduce VEGETATION NDVI by dynamic calculation of potential fragmentation.	New_NDVI(1km) = VEGETATION_NDVI × (individual pixel fragmentation value (obtained from figure 8), NDVI reduction, figure 4)

agricultural land predominantly in the centre and north-eastern portions of the scene.

5. Methods

5.1. *Single scene analysis*

As this paper is principally concerned with assessing the effect of fragmentation on the prediction of forest biomass accumulation, it is important to distinguish dense forest and scrub vegetation from cleared land, pasture and agriculture and all other land uses. Whilst the issue of fragmentation of agricultural and pasture areas by urban encroachment is important, it is not the focus of this study; therefore a simple forest/non-forest mask is all that is required. A simple forest mask was generated using spectral threshold values from the XS NDVI image (White *et al.* 1997). Thresholds were iteratively selected by comparing the extent of each forest mask to maps and local information. A NDVI value of 0.4 was used as the threshold on the XS image, with pixels having a NDVI value greater than 0.4 assigned as dense forest and scrub vegetation and less than 0.4 assigned as non-forest/sparse scrub. It is acknowledged that highly managed and irrigated agricultural areas may also be included in the dense vegetation class using this threshold. Applying this NDVI threshold to the XS image therefore allowed the development of a two-cover class map (forest/non-forest) and the boundaries between these classes were assumed to represent variations in the degree of forest fragmentation occurring in the landscape.

Chen (1999) described the mathematical basis of calculating bio-physical variables such as fPAR from mean reflectance for pixels with mixed sub-pixel land-cover classes. This mathematical step is required as the relationship between NDVI and the mean pixel reflectance in the red and NIR regions of the spectrum is non-linear. In a simple land-cover type situation with two classes, land-cover class A has a certain fraction, ω, of cover in a given pixel and therefore, by definition, land-cover class B will have the fraction, $1-\omega$, of cover in the same pixel. The mean pixel reflectance in the red and near-infrared regions of the spectrum in the broad-scale pixel is given by:

$$\rho_{\mathrm{r}} = \omega\rho_{r,\mathrm{A}} + (1-\omega)\rho_{\mathrm{r,B}} \tag{1}$$

$$\rho_{\mathrm{nir}} = \omega\rho_{\mathrm{nir,A}} + (1-\omega)\rho_{\mathrm{nir,B}} \tag{2}$$

where $\rho_{\mathrm{nir,A}}$ and $\rho_{\mathrm{r,A}}$ are reflectance values in the NIR and R regions of the spectrum for cover type A, respectively and $\rho_{\mathrm{nir,B}}$ and $\rho_{\mathrm{r,B}}$ are reflectance values in the NIR and R regions of the spectrum for cover type B, respectively.

The mean NDVI for the broad-scale pixel is therefore:

$$\mathrm{NDVI} = \frac{\omega\left(\rho_{\mathrm{nir,A}} - \rho_{\mathrm{r,A}}\right) + (1-\omega)\left(\rho_{\mathrm{nir,B}} - \rho_{\mathrm{r,B}}\right)}{\omega\left(\rho_{\mathrm{nir,A}} + \rho_{\mathrm{r,A}}\right) + (1-\omega)\left(\rho_{\mathrm{nir,B}} + \rho_{\mathrm{r,B}}\right)} \tag{3}$$

Using mean reflectance values from the XS image for the forest and non-forest class we can simulate the response of a mixed pixel using the equation of Chen (1999). Figure 3 indicates that the forest/non-forest example (▲) is strongly non-linear. NDVI values of 1 km pixels remain relatively stable for forest fragmentation values between 30 and 100% forest cover (figure 3). Once the 1 km pixel contains less than 30% forest area, the NDVI falls rapidly. The second curve (■) is the

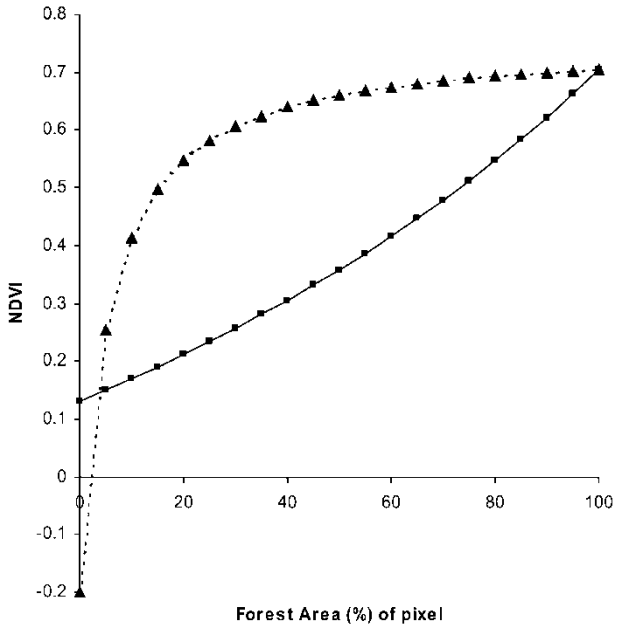

Figure 3. Variation in NDVI with a sub-pixel non-forest versus forest (▲) and forest versus inland water (■) fraction from Chen (1999) derived from SPOT XS imagery.

water–vegetation curve and is similar to the curve of Chen (1999) with an almost linear decrease in NDVI at the 1 km scale as the degree of water fragmentation increases.

5.2. *Physiological biomass modelling (using 3-PG simulations)*

The 3-PG model requires monthly climate surfaces, including maximum/minimum temperature (°C), total precipitation (mm), and daily average short-wave radiation ($MJ\,m^{-2}\ day^{-1}$). In addition, 3-PG requires basic information on soil fertility and soil water holding capacity. Coops *et al.* (2002) details the processing steps and data sources required for these data layers. When coupled with remotely sensed observations from the monthly VEGETATION data, 3-PG uses estimates of fPAR absorbed by the forest canopy to constrain carbon uptake. SPOT VEGETATION was calibrated with field-based estimates of fPAR obtained from the LAI-2000 (Li-Cor, Lincoln, Nebraska, USA) (Welles 1990, Welles and Norman 1991). Average hemispheric gap fraction was measured at 11 different locations across the North and South Islands of New Zealand in November 1997 on the assumption that average hemispheric gap fraction is a reasonable surrogate for fPAR and that clumping of foliage was random. Sites were selected to cover a gradient in elevation and precipitation with dominant forest and scrub types represented and a geographic extent ranging across the central South Island from the east to the west coast. A North Island site was also selected in the central volcanic plateau highlands where woody scrub vegetation has been previously studied (Scott *et al.* 2000). A simple linear adjustment was performed (Goward *et al.* 1994) on the SPOT VEGETATION November 1998 NDVI values to predict fPAR.

The developed equation was:

$$\text{fPAR} = (0.45 \times \text{NDVI}) + 0.61 \quad (4)$$

where NDVI is the SPOT-4 VEGETATION NDVI values between −1 and 1 ($n = 11$, $r^2 = 0.82$).

The 3-PG model, coupled with the broad-scale VEGETATION data, was run using standard parameter values and constants described in Coops *et al.* (2002). Detailed information on the selection of parameters for New Zealand forests are documented in White *et al.* (2000). The 3-PG simulation was run for a 12–month period from July 1998 to June 1999.

6. Results

6.1. *NDVI comparison between 1 km and 20 m images*

The 1 km grid over the VEGETATION image allows the 1 km NDVI value to be compared with the mean NDVI value for the same 1 km area on the XS 20 m image. The relationship between the 1 km NDVI (X axis) and the mean 20 m NDVI averaged over each 1 km grid-cell (Y axis) is shown in figure 4.

The slope of the relationship is 1.08, which differs significantly from 1 ($p < 0.05$), and the intercept is significantly different than 0 ($p < 0.05$), indicating a bias in the relationship between NDVI values measured at different spatial scales. The figure confirms the NDVI trajectories shown in figure 3, with broad-scale NDVI values overestimating the mean NDVI value of the high spatial resolution pixels aggregated up to 1 km pixels. At low NDVI values (NDVI = 0.1), mean 20 m NDVI values are overestimated by 28% at the 1 km scale; at higher NDVI values (NDVI = 0.7), mean 20 m NDVI values are overestimated by 22% at the 1 km scale.

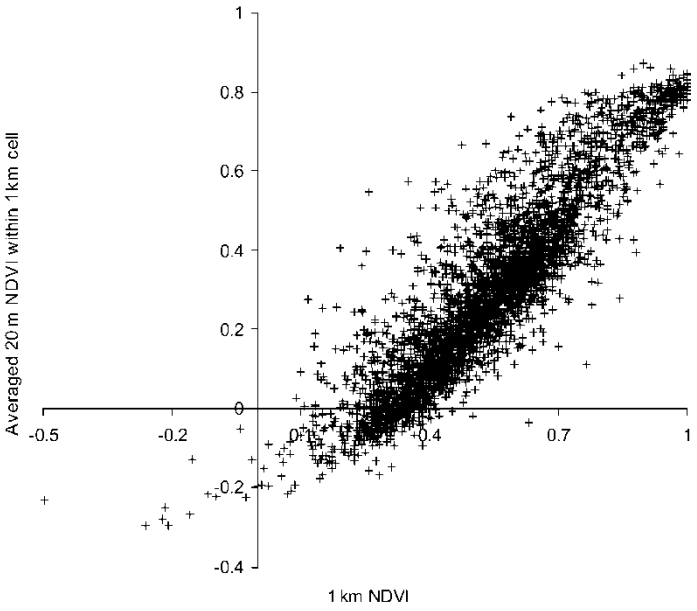

Figure 4. Relationship between 1 km VEGETATION NDVI values and 1 km NDVI values obtained by averaging 20 m pixels contained within the 1 km pixels.

6.2. *Image fragmentation*

As the single SPOT-4 VEGETATION and XS images were acquired simultaneously with identical atmospheric and vegetation conditions, it is possible to compare the areal extent of different land-cover types (or fragmentation of forest vegetation) in each 1 km pixel with the land cover in the 20 m pixels.

Using a threshold NDVI of 0.4 to distinguish forest from non-forest, we estimated fragmentation by comparing the NDVI value of the 1 km VEGETATION pixel against the proportion of 20 m forest non-forest cells within the same 1 km pixel (figure 5). VEGETATION pixels with a NDVI of 1.0 have virtually no fragmentation at the 20 m scale with 100% of the 20 m pixels having an NDVI greater than 0.4 (figure 5). Alternatively, a VEGETATION NDVI value of 0.8 indicates that the proportion of 20 m forest cells has fallen to 80% (or alternatively that 20% of the 20 m cells were non-forest (figure 5)). Likewise, VEGETATION NDVI equal to 0.6 had 38% forest at 20 m resolution and broad-scale 1 km pixels with an NDVI equal to 0.4 had only 11% forest at 20 m resolution. A number of models were fitted and a logarithmic function was found to be the most suitable (equation (5), figure 6, $r^2 = 0.97$).

$$\text{Proportion forest in 1 km cell} = 109.48 \ln(\text{NDVI}) + 103.52 \quad (5)$$

At low (0.4–0.48) and mid (0.7–0.9) NDVI values, fragmentation was slightly overestimated, while between 0.48 and 0.68 fragmentation was slightly underestimated (figure 7). This relationship (figures 8 and 9) provides a link between the broad-scale VEGETATION NDVI values frequently used in production-efficiency models with fine-scale contextual information in each pixel.

Figure 8(*a*) shows the spatial extrapolation of the logarithmic equation (5) using the VEGETATION 1 km NDVI data as the input. Pixels that are predicted to contain both forest and non-forest classes are shown as black and pixels that are predicted to be 'pure' are shown as white (figure 8(*a*)). The figure shows pixels in the

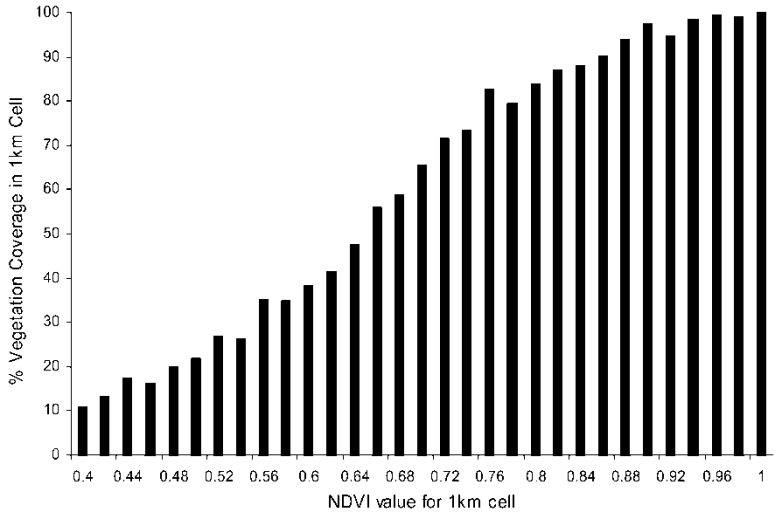

Figure 5. Estimated degree of fragmentation (*y*-axis) within 1 km VEGETATION pixels, stratified by NDVI (*x*-axis) using 20 m forest and non-forest cells (i.e. % of 1 km cell vegetated) using simultaneously acquired SPOT-4 imagery for New Zealand.

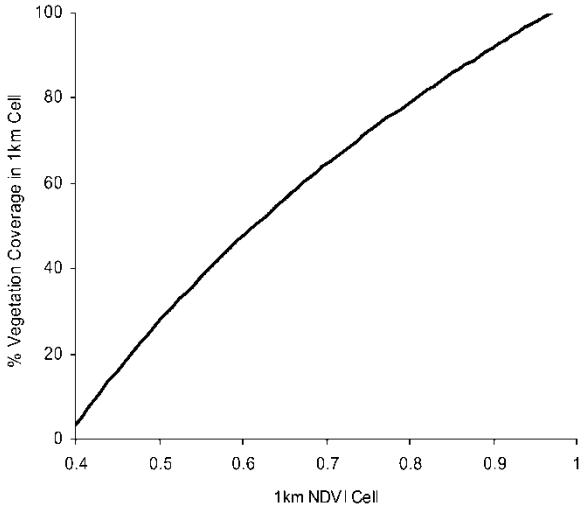

Figure 6. Relationship between 1 km VEGETATION NDVI and degree of fragmentation (using a logarithmic function) within 1 km VEGETATION pixels.

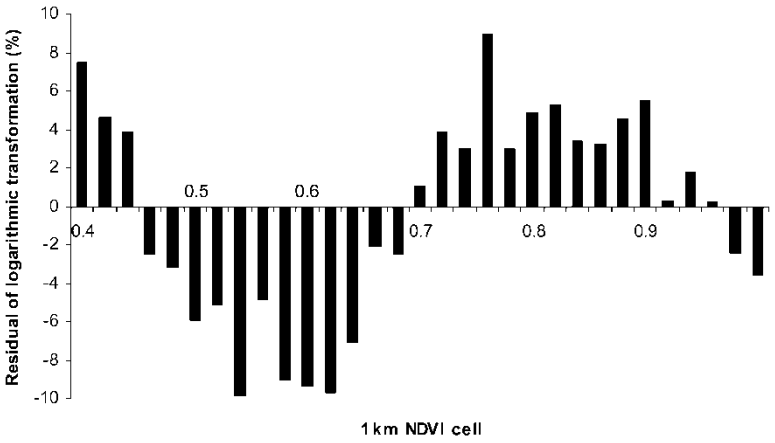

Figure 7. Residuals of the fitted logarithmic function depicted in figure 6.

centre of large areas of forest are white indicating they are completely filled with forest vegetation similar to the NDVI image (figure 2(*b*)); however, the logarithmic transform provides an indication of the sub-pixel fragmentation with the edges of the forest being predicted as having more fragmentation and are thus darker.

Figure 8(*b*) transforms figure 8(*a*) using figure 6 and provides an indication of the reduction in NDVI that is expected based on the degree of fragmentation within the pixel. If the reduction is small then it indicates that the predicted value is similar to the actual broad-scale value (white in figure 10(*b*)). If the value is large then there is significant difference between the actual NDVI value and the predicted value (if the pixel was 100% filled with forest) (black in figure 8(*b*)). The figure shows the large patches of forest are bright with high values indicating no significant change predicted in NDVI based on sub-pixel fragmentation. By contrast, the areas along

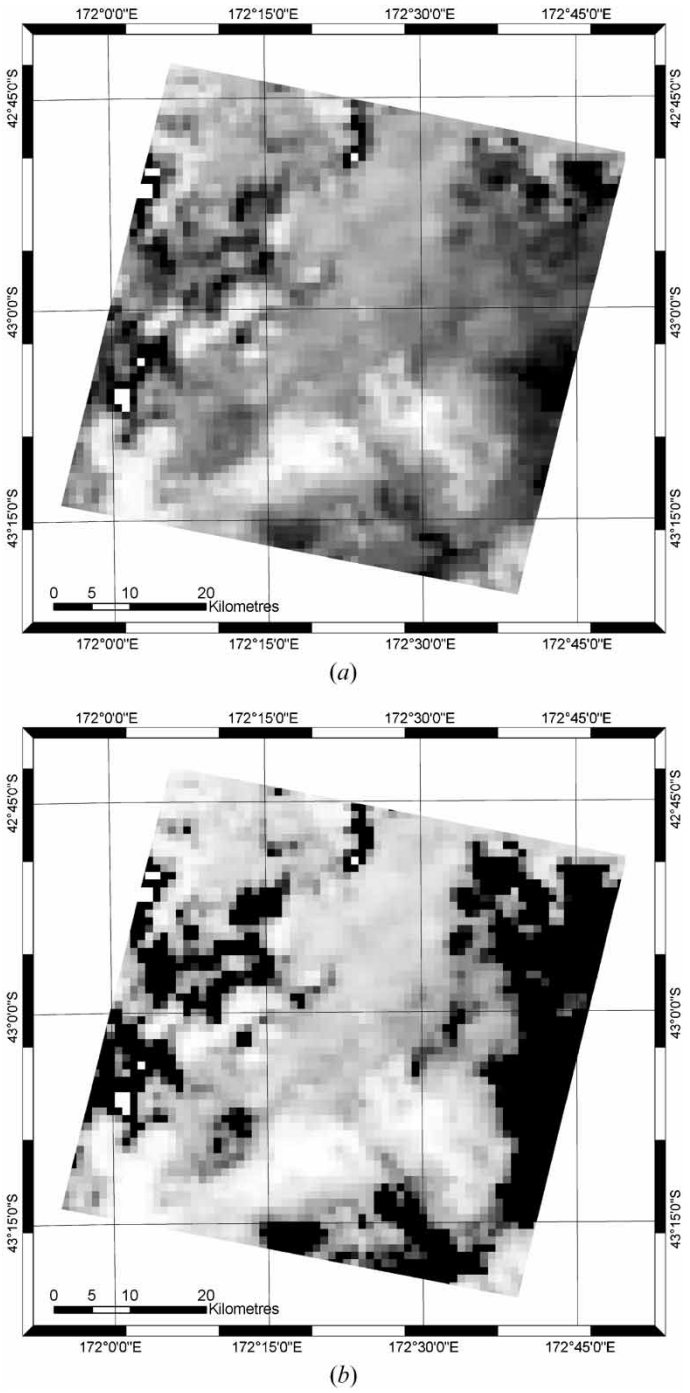

Figure 8. (*a*) Predicted sub-pixel forest/non-forest fragmentation within 1 km SPOT VEGETATION image using SPOT XS 20 m forest/non-forest classification (pixels predicted to contain both forest and non-forest are shown as black, and pixels predicted to be 'pure' are shown as white). (*b*) Transformation of (*a*) to predicted variation in NDVI based on pixel fragmentation. White indicates small NDVI reduction due to fragmentation, black indicates high degree of fragmentation correction.

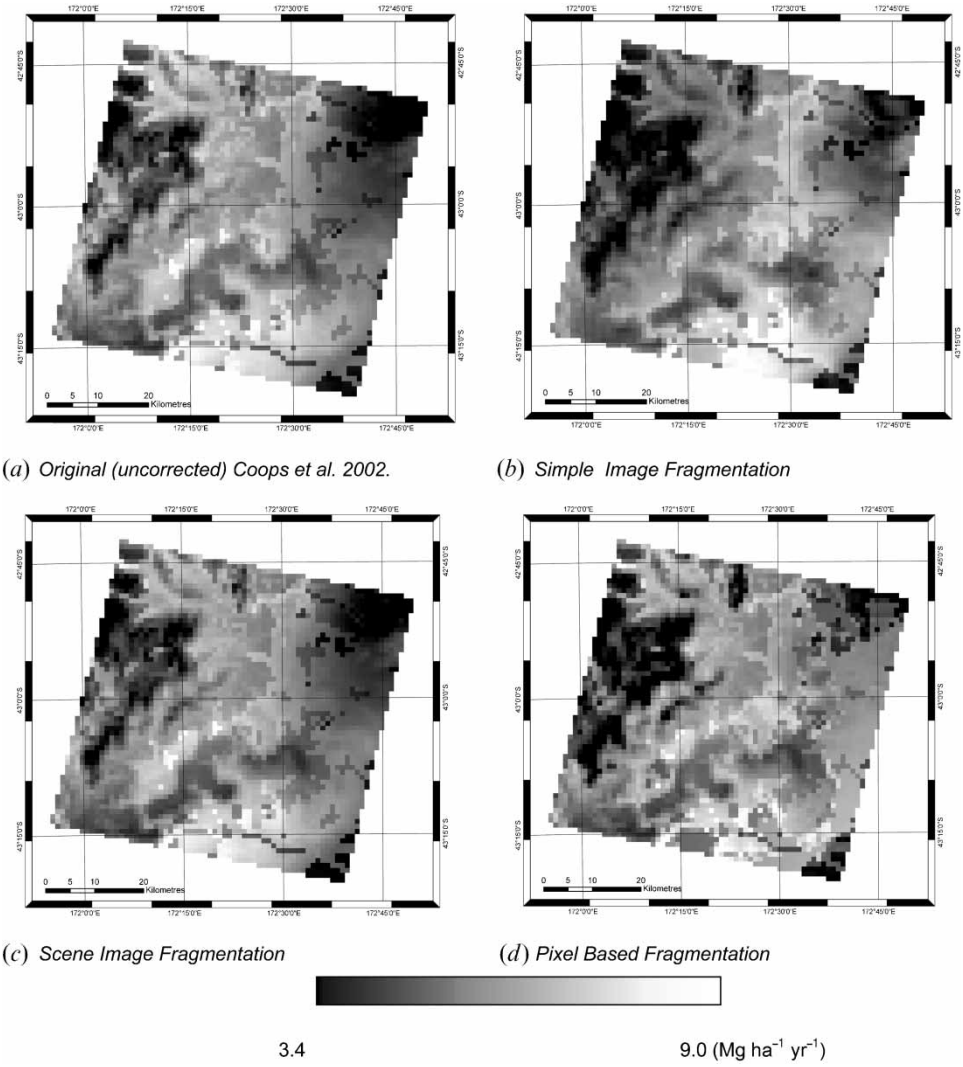

Figure 9. Predicted NPP_A for (*a*) the uncorrected NDVI images, and (*b*)–(*d*) the three different methodologies presented in table 1.

the west of the study area that have significant forest fragmentation are black, indicating significant reduction in NDVI based on predicted fragmentation. Likewise, high variability in the pasture areas in the east of the study area (figure 2(*a*)) (indicating patches of native forest vegetation) also appear to be highly fragmented.

6.3. *Proposed scaling alternatives*

Based on these results, we propose three methods by which the 1 km VEGETATION pixel and the fine-scale SPOT XS image can be used to provide information on forest fragmentation, and its subsequent effect on broad-scale estimates of NDVI, fPAR and, ultimately, simulated NPP_A (table 1).

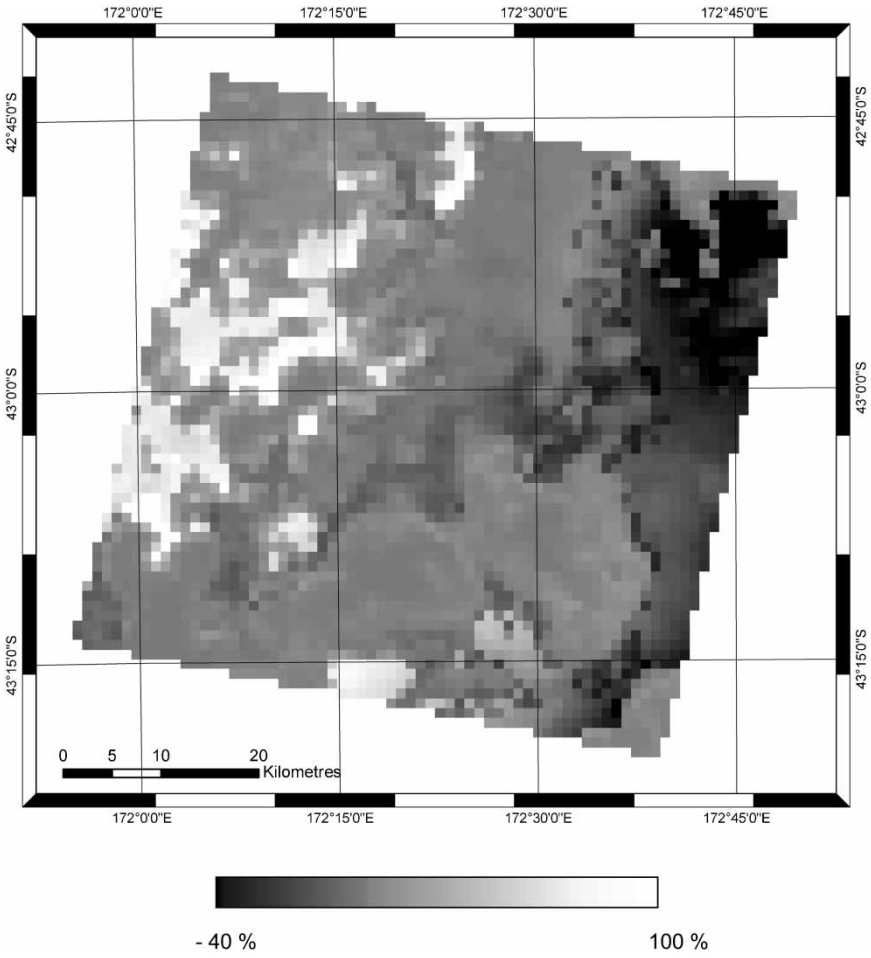

Figure 10. Difference in NPP_A between 3-PG predictions based on uncorrected NDVI images and NDVI images corrected using the pixel-based correction method.

1. Simple image fragmentation. A simple regression relationship that accounts for the over-estimation of broad-scale NDVI values when compared with the aggregated 20 m NDVI values can be derived by comparing sample areas using both 1 km and 20 m data. From this a simple conversion can be derived which adjusts the broad 1 km scale NDVI values (figure 4). This method applies the simple shift to all broad-scale NDVI values, and simply accounts for shifts in the NDVI regardless of land-cover types present. This approach requires limited information on the fine-scale variation in the scene. General equations like this could be generated at selected sites over the entire country and applied to remove any broad bias in broad-scale NDVI values.

2. Scene-based fragmentation. This adjustment utilizes the contextural information of the fine-scale NDVI scene by computing the degree of fragmentation for the whole scene at the 1 km pixel size and then adjusting the 1 km NDVI value by an amount according to figure 3. To do this requires an *a priori* assumption as to the

two major contrasting land-cover types in the image. If, such as in this case, a combination of forest and non-forest land-cover types exists, figure 3 indicates that a mean 1 km pixel with 100% forest vegetation has a NDVI equal to 0.74. If the mean degree of fragmentation for the image, at the 1 km scale, was 78%, the mean corrected NDVI value is 0.68 resulting in an NDVI reduction of 0.1 NDVI units or 12%. The benefit of this technique, compared to the previous one, is that it allows the actual fragmentation values of the landscape to be explicitly accounted for in the study area.

3. Pixel-based fragmentation. The final method allows the actual amount of fragmentation within each 1 km cell to be calculated and the NDVI adjusted accordingly. The developed logarithmic relationship (figure 6) that predicts the amount of fragmentation in each 1 km pixel based on the VEGETATION NDVI value is developed based on inter-comparison between 1 km and 20 m data. Using the predicted percent fragmentation for each pixel, the reduction in NDVI can be derived from figure 3 as before. The benefit of this method over the previous ones is that, using the logarithmic relationship specifically developed for these two scenes, the broad-scale image can be dynamically adjusted on an individual pixel basis using the 1 km NDVI values.

Using these three methods for correcting the coarse-scale NDVI based on fragmentation (table 1), we simulated NPP_A for the area covered by the high resolution SPOT-XS image using the 3-PG model (figure 9). Figure 9(*a*) shows the uncorrected prediction of NPP_A. As figure 9 indicates, the prediction of NPP_A based on the different correction methods appear similar (figure 9(*b*)–(*d*)), indicating similar predictions of NPP_A over the area. Importantly, a number of environmental factors such as species adaptation to temperature, fertility and water use are all used in the prediction of NPP_A using 3-PG. As a result patterns in NPP_A will vary compared to the input NDVI images. The difference between the original and the simple image-based correction (the simple adjustment of VEGETATION NDVI by a scaling factor) is minor and simply reduces the overall fPAR of the scene by a constant amount. The scene-based fragmentation method also reduced the scene fPAR by a constant fraction, which is less than the overall image adjustment (NDVI reduction of 12% versus 22%) resulting in a mean prediction of NPP_A lying between the original and the simple adjustment method. The final pixel-based fragmentation method uses individual pixel-based calculations of fragmentation and reduces each VEGETATION NDVI pixel by the correct amount and thus produces a different result (figure 9(*d*)). Much of the agricultural regions have reduced and more constant NPP_A values compared with the original, uncorrected simulations (figure 9(*a*)). This is due to the predicted fragmentation effect removing much of the variation in the eastern portion of the study area (figure 9(*a*)). In addition, the prediction of NPP_A appears less smooth than the uncorrected image with more high frequency information along the boundaries between land uses with areas where fragmentation clearly exists having less NPP_A than the original uncorrected predictions. Figure 10 shows the difference between the predictions of NPP_A using the uncorrected and the pixel-based fragmentation method. White pixels indicate a greater prediction of NPP_A from the uncorrected NDVI imagery and dark pixels indicates a greater prediction of NPP_A. The difference image again shows areas where mixed pixels are likely to occur having significantly reduced

NPP_A by up to 100%. In contrast, within large areas of forest the difference between the two methods is much smaller.

We assessed statistical differences between the three methods and the original simulations using a one-way ANOVA with a Tukey's HSD *post hoc* analysis (figure 11). The ANOVA indicated that the original (uncorrected) simulation was significantly ($p < 0.05$) different from all fragmentation-corrected predictions. The ANOVA also indicated that the simple image-based fragmentation technique and the scene-based fragmentation (the two methods involving a simple rescaling of the NDVI) were not significantly different from each other however were different from the pixel-based fragmentation method.

7. Discussion and conclusion

When modelling ecosystem processes, aggregation of surface properties either through the inherent restrictions of sensor resolution or by direct data manipulation results in overestimation of vegetation productivity (White and Running 1994, Pierce and Running 1995). Landscapes are generally heterogeneous at spatial scales finer than most global observing satellites. Contextural characteristics of high spatial resolution data are useful for adjusting vegetation indices that are used to estimate intercepted radiation by vegetation with varying absorption properties, biomass and phenology. Therefore, the effect of spatial resolution on the prediction of forest biophysical properties and land classes has been an area of ongoing study in the remote sensing community (Moody and Woodcock 1994, Mayaux and Lambin 1995). This is particularly important for improving estimates of carbon budgets at different spatial scales, as remote sensing is frequently used to either map vegetation classes or quantify forest biophysical properties such as fPAR.

Moody (1998) attributes these resolution effects to (a) a tendency for dominant

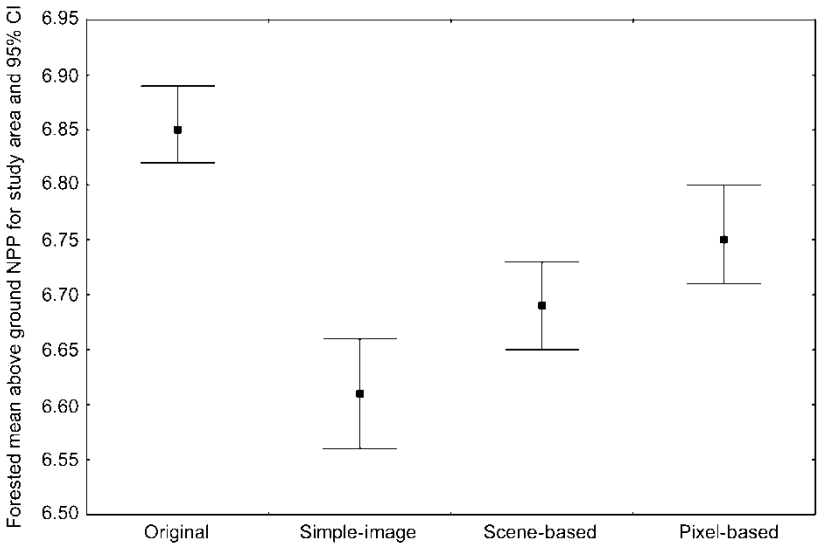

Figure 11. Differences (mean and 95% confidence intervals (CI)) in NPP_A for forested pixels in the study area based on the three different correction methods. (1) Original, (2) simple image fragmentation, (3) scene-based fragmentation and (4) pixel-based fragmentation.

classes to increase their dominance, and secondary classes to decrease their dominance at successively coarser resolutions; (b) modulations of this effect related to the spatial organization of the classes in the landscape and (c) the effects caused by the mixing of class spectra from the surface via the atmosphere to the sensor. Moody (1998) found that coarse-resolution data consistently overestimated biophysical variables compared with 30 m Landsat TM imagery. However, in that study Landsat TM imagery was used to generate the coarse-resolution imagery to ensure coincident imagery acquisition. As a result, significant spatial averaging was required to generate coarse imagery from the original Landsat TM 30 m cells, which may not represent the coarse-scale estimates of landscape conditions.

A unique aspect of this study was that we used coincident 20 m and 1 km imagery from the SPOT VEGETATION and XS instruments, providing an important dataset to examine this scaling issue. Issues of differences in vegetation condition and structure, satellite position and sun angle can be ignored when using coupled data from SPOT-4 making these results more robust than those from TM- and AVHRR-driven data examples (Moody 1998). Like the Moody (1998) study, we found that a potential exists in the overestimation of variables (using 1 km resolution data) which are used to drive bio-physical models compared with 20 m XS imagery.

Previous studies have estimated the sensitivity of ecosystem and climate models to errors caused by fragmentation and scaling area estimates (Moody and Woodcock 1994, Moody 1998). These errors can lead to biases in model parameterization and simulated results, increasing uncertainty in model predictions above that inherent to the model itself. Our results support the concept that sub-pixel fragmentation significantly alters coarse-scale predictions. We found that predictions of fPAR could vary by as much as 45% of the 'true' value for coarse pixels with two distinct land-cover classes (figure 10). The degree of bias in the predictions, whilst large, is comparable with the estimates predicted by Chen (1999) and Moody (1998). In the 3-PG model, fPAR is the scaled variable based on remote sensing observations. It is possible for a variety of other variables to be tested similarly, including temperature, vegetation class and leaf area index.

As the complexity of each correction method increases, the generality of application may go down. The first technique (simple image fragmentation), whilst the most crude, provides a general indication of the required adjustment of 1 km NDVI values to more accurately reflect the fine-resolution values. This regression equation could be developed for a region or from a number of selected pooled scenes and used without further calibration. In the second method (scene-based fragmentation) the XS image scene may not necessarily be required to predict the amount of forest fragmentation as it could be broadly estimated from land-cover mapping or from a number of different satellite or mapping sources. In the final method (pixel-based fragmentation), both the 1 km (VEGETATION) and the 20 m (XS) scenes are required in order to derive figures 3 and 6.

The mean NPP_A of the study area using the three correction methods is significantly different from the original, uncorrected modelling approach, with results showing the effect of fragmentation occurring at very fine scales over the 60 km × 60 km study area. Figure 10 indicates that significant pixel-based variation does occur over the study area with variation by as much as 100% of the

uncorrected values over long forest edges and regions with significant forest–agriculture boundaries.

Acknowledgments

This research was undertaken at Landcare Research New Zealand, and supported in part by the New Zealand Ministry for the Environment and the Foundation for Research, Science, and Technology (CO9807). We thank Dr James Shepherd for the pre-processed SPOT-4 imagery used in this project. Dr Brendan Mackey and Mr Andrew Loughead provided valuable comments on the draft manuscript. Additional support was provided by the Department of Biology, Baylor University, USA and The Woods Hole Research Center, USA. We acknowledge Dr Joe Landsberg (CSIRO Land and Water) and Prof. Richard Waring (Oregon State University) who developed the original 3-PG framework and thank them for their advice and valuable discussions on the use and application of the model. The paper also benefited from comments by the anonymous reviewers.

Additional information on the 3-PG model and free code is available at: http://www.ffp.csiro.au/nfm/mdp/

References

AHERN, F. J., BROWN, R. J., CIHLAR, J., GAUYHIER, R., MURPHY, J., NEVILLE, R. A., and TEILLET, P. M., 1987, Radiometric correction of visible and infrared remote sensing data at the Canada Centre for Remote Sensing. *International Journal of Remote Sensing*, **8**, 1349–1376.

CHEN, J. M., 1999, Spatial scaling of a remotely sensed surface parameter by contexture. *Remote Sensing of Environment*, **69**, 30–42.

COLLINGE, S. K., 1996, Ecological consequences of habitat fragmentation: implications for landscape architecture and planning. *Landscape and Urban Planning*, **36**, 59–77.

COOPS, N. C., WARING, R. H., and LANDSBERG, J. J., 1998, Assessing forest productivity in Australia and New Zealand using a physiologically-based model driven with averaged monthly weather data and satellite derived estimates of canopy photosynthetic capacity. *Forest Ecology and Management*, **104**, 113–127.

COOPS, N. C., WHITE, J. D., and SCOTT, N. A., 2002, Assessment of regional forest and scrub productivity using a coupled vegetation process model with remote sensing. *GeoCarto*, **17**, 1–12.

FORMAN, R. T. T., and GODRON, M., 1986, *Landscape Ecology* (New York: John Wiley).

GOETZ, S. J., PRINCE, S. D., GOWARD, S. N., THAWLEY, M. M., and SMALL, J., 1999, Satellite remote sensing of primary production: an improved production efficiency modelling approach. *Ecological Modelling*, **122**, 239–255.

GOWARD, S. N., WARING, R. H., DYE, D. G., and YANG, J., 1994, Ecological remote sensing at OTTER: satellite macroscale observations. *Ecological Applications*, **4**, 322–343.

HALL, G. M. K., WISER, S. K., ALLEN, R. B., BEETS, P. N., and GOULDING, C. J., 2001, Strategies to estimate national forest carbon stocks from inventory data: the 1990 New Zealand baseline. *Global Change Biology*, **7**, 389–403.

LANDSBERG, J. J., and WARING, R. H., 1997, A generalised model of forest productivity using simplified concepts of radiation-use efficiency, carbon balance and partitioning. *Forest Ecology and Management*, **95**, 209–228.

MATHER, P. M., 1987, *Computer Processing of Remotely Sensed Images* (New York: Wiley).

MAYAUX, P., and LAMBIN, E., 1995, Estimation of tropical forest area from coarse spatial resolution data: a two step corrective function for proportional errors. *Remote Sensing of Environment*, **53**, 1–6.

MEURK, C. D., and SWAFFIELD, S. R., 2000, A landscape ecological framework for indigenous regeneration in rural New Zealand–Aotearoa. *Landscape and Urban Planning*, **50**, 129–144.

MOODY, A., 1998, Using landscape spatial relationships to improve estimates of land-cover area from coarse resolution remote sensing. *Remote Sensing of Environment*, **64**, 202–220.

MOODY, A., and WOODCOCK, C. E., 1994, Scale-dependent errors in the estimation of land cover properties—implications for global land cover datasets. *Photogrammetric Engineering and Remote Sensing*, **60**, 585–594.

MURCIA, C., 1995, Edge effects in fragmented forests: implications for conservation. *Trends in Ecology and Evolution*, **10**, 58–62.

NEWSOME, P. F. J., 1987, The vegetation cover of New Zealand. National Water and Soil Conservation Authority, Ministry of Works and Development, Water and Soil Miscellaneous Publication No. 112, 153 pp.

PIERCE, L. L., and RUNNING, S. W., 1995, The effects of aggregating sub-grid land surface variation on large-scale estimates of net primary productivity. *Landscape Ecology*, **4**, 239–253.

SCOTT, N. A., WHITE, J. D., TOWNSEND, J., WHITEHEAD, D., LEATHWICK, J., HALL, G., MARDEN, M., ROGERS, G., WATSON, A. J., and WHALEY, P., 1999, Carbon and nitrogen distribution and accumulation in a New Zealand scrubland ecosystem. *Canadian Journal Forest Research*, **30**, 1246–1255.

WELLES, J. M., 1990, Some indirect methods of estimating canopy structure. *Remote Sensing Reviews*, **5**, 31–43.

WELLES, J. M., and NORMAN, J. M., 1991, Instrument for indirect measurement of canopy architecture. *Agronomy Journal*, **83**, 818–825.

WHITE, J. D., and RUNNING, S. W., 1994, Testing scale dependent assumptions in regional ecosystem simulations. *Journal of Vegetation Science*, **5**, 6867–6702.

WHITE, J. D., RUNNING, S. W., NEMANI, R., KEANE, R. E., and RYAN, K. C., 1997, Measurement and remote sensing of LAI in Rocky Mountain montane ecosystems. *Canadian Journal of Forest Research*, **27**, 1714–1727.

WHITE, J. D., COOPS, N. C., and SCOTT, N. A., 2000, Estimates of New Zealand forest and scrub biomass from the 3-PG model. *Ecological Modeling*, **131**, 175–190.

YOUNG, A., and MITCHELL, N., 1993, Microclimate and vegetation edge effects in a fragmented podocarp-broadleaf forest in New Zealand. *Biological Conservation*, **67**, 63–72.